Comparison of Magnetic Resonance Imaging of Aortic Valve Stenosis and Aortic Root to Multimodality Imaging for Selection of Transcatheter Aortic Valve Implantation Candidates

Bernard P. Paelinck, MD, PhD[a,*], Paul L. Van Herck, MD, PhD[a], Inez Rodrigus, MD, PhD[b], Marc J. Claeys, MD, PhD[a], Jean-Claude Laborde, MD[c], Paul M. Parizel, MD, PhD[d], Christiaan J. Vrints, MD, PhD[a], and Johan M. Bosmans, MD, PhD[a]

The purpose of the present study was to compare the aortic valve area, aortic valve annulus, and aortic root dimensions measured using magnetic resonance imaging (MRI) with catheterization, transthoracic echocardiography (TTE), and transesophageal echocardiography (TEE). An optimal prosthesis–aortic root match is an essential goal when evaluating patients for transcatheter aortic valve implantation. Comparisons between MRI and the other imaging techniques are rare and need validation. In 24 consecutive, high-risk, symptomatic patients with severe aortic stenosis, aortic valve area was prospectively determined using MRI and direct planimetry using three-dimensional TTE and calculated by catheterization using the Gorlin equation and by Doppler echocardiography using the continuity equation. Aortic valve annulus and the aortic root dimensions were prospectively measured using MRI, 2-dimensional TTE, and invasive aortography. In addition, aortic valve annulus was measured using TEE. No differences in aortic valve area were found among MRI, Doppler echocardiography, and 3-dimensional TTE compared with catheterization ($p = NS$). Invasive angiography underestimated aortic valve annulus compared with MRI ($p < 0.001$), TEE ($p < 0.001$), and 2-dimensional TTE ($p < 0.001$). Two-dimensional TTE tended to underestimate the aortic valve annulus diameters compared to TEE and MRI. In contrast to 2-dimensional TTE, 3 patients had aortic valve annulus beyond the transcatheter aortic valve implantation range using TEE and MRI. In conclusion, MRI planimetry, Doppler, and 3-dimensional TTE provided an accurate estimate of the aortic valve area compared to catheterization. MRI and TEE provided similar and essential assessment of the aortic valve annulus dimensions, especially at the limits of the transcatheter aortic valve implantation range. **(Am J Cardiol 2011;xx:xxx)**

Magnetic resonance imaging (MRI) has the unique potential of 3-dimensional (3D) cardiac imaging and analysis with great accuracy and reproducibility without the need for potential nephrotoxic contrast media. MRI permits visualization of the aortic valve and root despite the presence of calcifications. However, comparisons between MRI and other imaging techniques are rare. Because the results among imaging techniques can be conflicting,[1,2] the potential role of MRI in relation to other imaging techniques to assess the technical feasibility of transcatheter aortic valve implantation needs additional validation. We aimed to compare the aortic valve area and aortic root dimensions using MRI and a multimodality imaging approach including Doppler, 2-dimensional (2D) transthoracic echocardiography (TTE), 3D TTE and transesophageal echocardiography (TEE), and catheterization.

Methods

Consecutive high-risk elderly symptomatic patients with severe aortic stenosis who had been referred for clinically indicated heart catheterization and preprocedural transcatheter aortic valve implantation screening were prospectively studied. The aortic valve area was determined using steady-state free precession MRI and direct planimetry using 3D TTE and calculated by cardiac catheterization using the Gorlin equation[3] and Doppler echocardiography using the continuity equation.[4] The diameter of aortic valve annulus (at midsystole at the insertion of the leaflets), aortic sinus, sinotubular junction, and ascending aorta (4.5 cm above aortic valve annulus; Figure 1) were measured using steady-state free precession MRI and compared to 2D TTE, TEE, and invasive aortography. The diameter of the left ventricular outflow tract was measured using steady-state free precession MRI and compared to 2D TTE. In addition, the diameter of aortic valve annulus was measured using TEE (Figure 1).

Departments of [a]Cardiology, [b]Cardiac Surgery, and [d]Radiology, University Hospital, Antwerp, Belgium; and [c]Royal Brompton Hospital, London, United Kindgom. Manuscript received December 30, 2010; manuscript received and accepted February 24, 2011.

Dr. Laborde is a consultant for Medtronic, and Drs. Laborde and Bosmans are clinical proctors for Medtronic CoreValve, Medtronic, Inc., Minneapolis, Minnesota.

*Corresponding author: Tel: (+32) 3-821-4182; fax: (+32) 3-825-0848.

E-mail address: Bernard.Paelinck@uza.be (B.P. Paelinck).

0002-9149/11/$ – see front matter
doi:10.1016/j.amjcard.2011.02.348

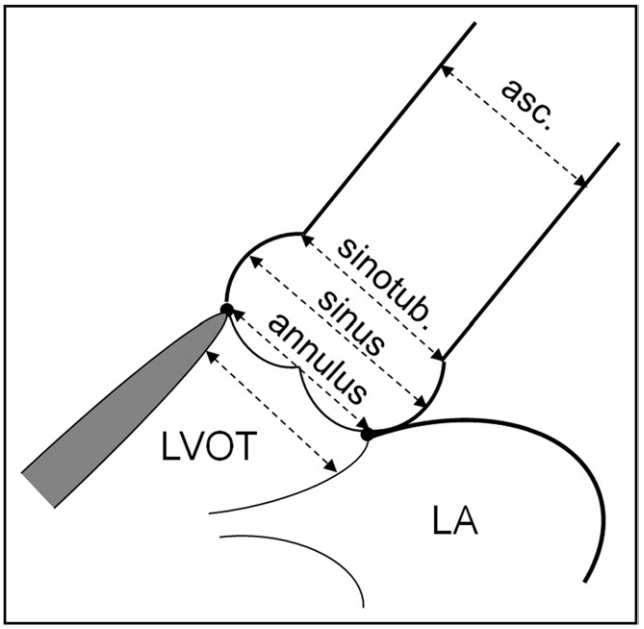

Figure 1. Schematic view of left ventricular outflow tract and aortic root. Schematic 3-chamber view (acquired by 2D TTE, TEE, and MRI) with diameter of left ventricular outflow tract (LVOT), aortic valve annulus, aortic sinus, sinotubular junction, and ascending aorta (4.5 cm distal from aortic annulus). Asc. = ascending aorta; LA = left atrium; sinotub = sinotubular junction; 2D = two-dimensional.

Noninvasive measurements were performed by 2 independent readers (B.P.P. and P.V.H.) who were unaware of the invasive measurements and had extensive experience with the analysis of steady-state free precession MRI and 2D and 3D echocardiography. Two independent observers (C.J.V. and J.M.B.), who were unaware of the noninvasive measurements, performed the invasive measurements. All measurements were done off-line and repeated ≥3 times. The mean value of these measurements was used for analysis. The medical ethical committee of the Antwerp University Hospital approved the protocol, and all patients gave written informed consent before participation.

Echocardiography was performed with an iE33 phased-array scanner (Philips Medical Systems, Andover, Massachusetts) with an S5-1 5 to 1 MHz extended frequency range transducer for 2D imaging and Doppler, and an X3-1 broadband xMatrix array transducer for 3D imaging. Three consecutive cardiac cycles were acquired and stored for each parameter. The diameter of the left ventricular outflow tract, aortic valve annulus, aortic sinus, sinotubular junction, and ascending aorta was measured from the parasternal long-axis view (Figures 1 and 2). Three-dimensional echocardiographic volumes incorporating the aortic valve were acquired from the parasternal window with electrocardiographic gating and breath holding (during 8 heartbeats). Off-line analysis using dedicated software (Qlab, version 7.0, 3D Q-Advanced, Philips, Maastricht, The Netherlands)

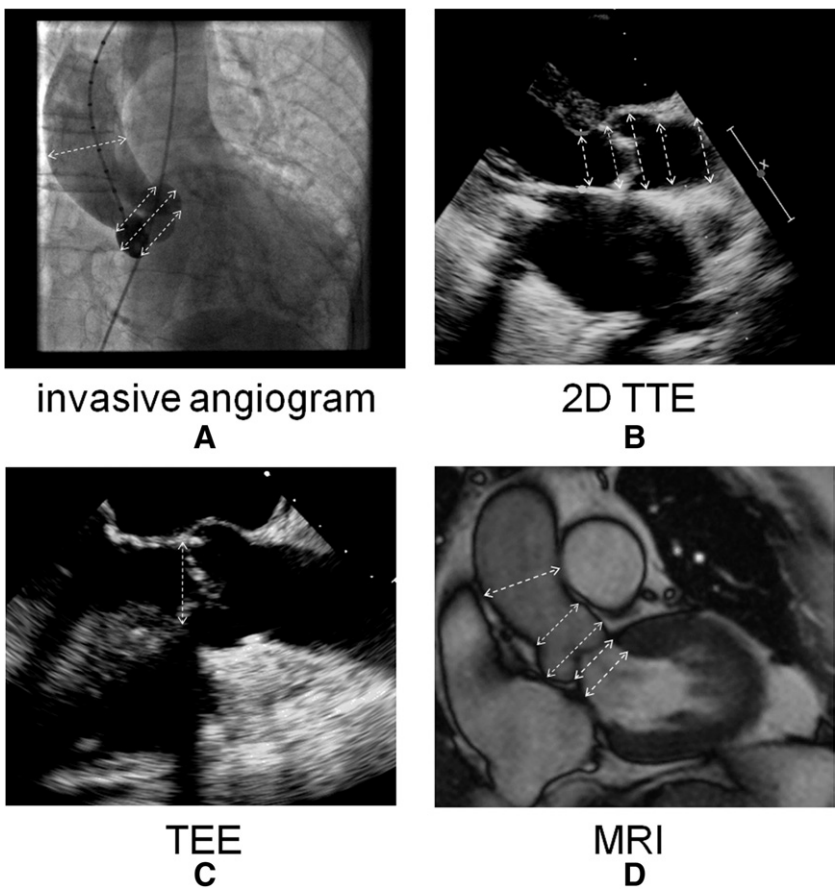

Figure 2. Multimodality imaging of aortic root. Example of *(A)* invasive angiogram and 3-chamber view by *(B)* 2D TTE, *(C)* TEE, and *(D)* MRI for measurement of aortic valve annulus, aortic sinuses, sinotubular junction. and ascending aorta.

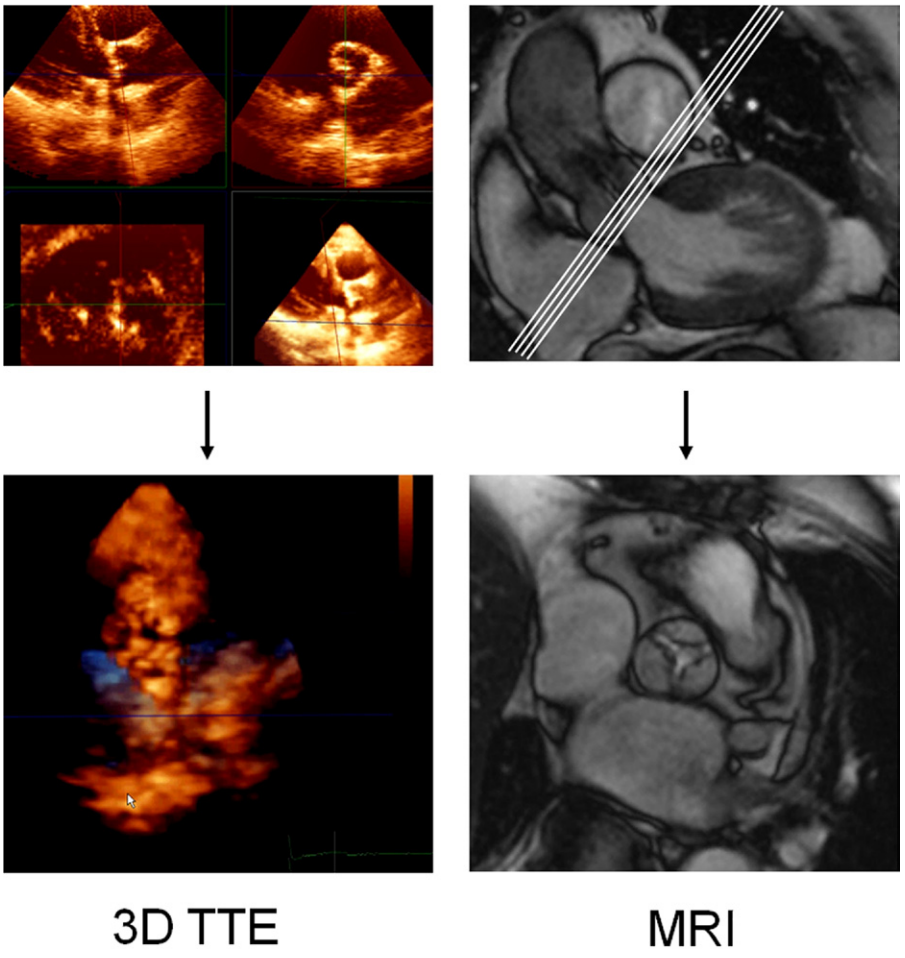

Figure 3. Planimetry of aortic valve. *(Left)* Short-axis 3D TTE of aortic valve at maximum opening during systole intended for planimetry. From 3D data set, orthogonal long-axis views of aortic valve were extracted. Cross-sectional view of aortic valve obtained by additional perpendicular plane on these long-axis views. *(Right)* MRI slices at level of aortic valve. Corresponding MRI scan of aortic valve at maximum opening during systole intended for planimetry.

was performed by an investigator, who was unaware of the results of the other measurements. Direct planimetry of the aortic valve was done after cropping and by alignment of the short-axis plane along the narrowest orifice in systole using the orthogonal long-axis plane (Figure 3).

The subjects were examined using a Sonata MRI scanner (Siemens, Erlangen, Germany) and a commercially available 12-channel body array surface coil. Retrospective electrocardiographically triggered breath-hold steady-state free precession (true fast imaging with steady state precession) imaging of the heart was performed. The imaging parameters were repetition time 3.2 ms, echo time 1.6 ms, 8-mm section thickness, 2-mm interslice gap, 240 × 256 matrix, 380 × 380 mm field of view, 1.6 × 1.5 mm in-plane spatial resolution, and 65° flip angle. The temporal resolution was 40 ms. The entire heart was imaged in the short-axis orientation, as described previously.[5] For determination of the aortic valve annulus and aortic root dimensions, a long-axis cine image was acquired by cutting the plane of the left ventricular outflow tract and the posterolateral wall in the most basal short-axis image (Figure 2). Using this 3-chamber view, multiple (average of 4) contiguous breath-hold true fast imaging with steady state precession cine images of the aortic valve starting at the left ventricular outflow tract and ending at the valve tips, were acquired perpendicular to the aortic root (slice displacement 2 mm). Planimetry for the assessment of the aortic valve area was obtained by delineating the edges of the maximum opening of the aortic valve during systole on each image slice using ARGUS software (Siemens, Erlangen, Germany; Figure 3). The smallest aortic valve area was used in the analysis.

Multiplanar TEE was performed using a Philips iE33 phased-array scanner, with a 7.5-MHz multiplanar probe. For optimal measurement of the aortic valve annulus, the zoomed long-axis view of the ascending aorta and left ventricular outflow tract (usually 110° to 150°) at midsystole was used (Figure 2).

Invasive measurements were performed using a 5Fr marked pigtail catheter positioned in the noncoronary sinus. The angiographic view, looking perpendicular to the aortic valve annulus in which the 3 coronary cusps were perfectly lined in 1 plane, was selected for the measurements. The aortic valve annulus, defined as the angiographic attachment point of the calcified valve leaflets, was measured during systole. The maximum diameter of the coronary sinuses, height of the sinuses, and diameter of the sinotubular junc-

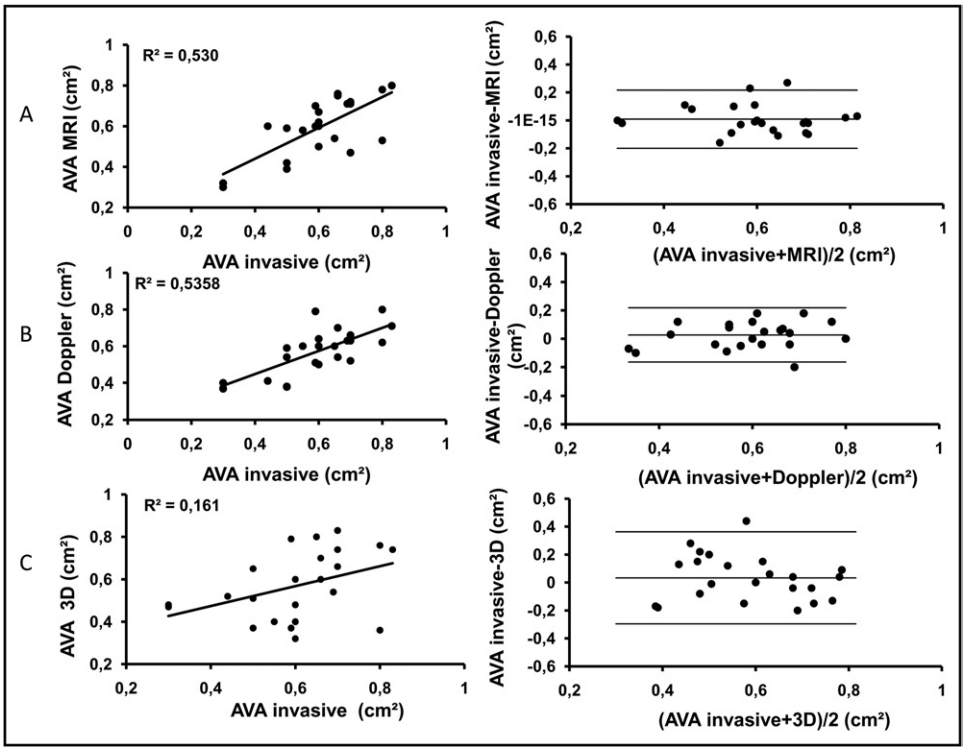

Figure 4. Correlations between MRI planimetry and multimodality measurement of aortic valve area. Correlation between calculated aortic valve area by catheterization and aortic valve area by MRI planimetry *(A)*, Doppler *(B)*, and 3D TTE planimetry *(C)*. Bland-Altman plots of difference between calculated aortic valve area by catheterization and MRI planimetry *(A)*, Doppler *(B)*, and 3D TTE planimetry *(C)*. Horizontal lines show mean difference between 2 methods ± 2 SDs.

tion and of the basal aorta 4.5 cm above the aortic valve annulus were measured, all with use of the marked pigtail as a reference (Figure 2).

Data are expressed as the median and range. The normality of the data was verified with a Shapiro-Wilk test. Differences between normally distributed measurements were tested with repeated measurements analysis of variance. A Bonferroni correction was applied for the pairwise comparisons (post hoc test). A Friedman test was used to assess differences between non-normally distributed measurements. A Wilcoxon signed rank test with Bonferroni correction was applied as the post hoc test. An analysis of the limits of agreement was evaluated in accordance with Bland and Altman.[6] The intra- and interobserver reproducibility was assessed in 10 randomly selected patients and is expressed as the mean difference ±2 SDs. The statistical analysis was performed using the Statistical Package for Social Sciences, version 17.0 (SPSS, Chicago, Illinois). Significance was defined as $p < 0.05$.

Results

A total of 24 consecutive high-risk elderly symptomatic patients (8 men and 16 women, mean age 83.5 years, range 67 to 88) with severe aortic stenosis were included in the present study. The image quality of MRI and 2D and 3D TTE was considered sufficient for analysis in all patients. In 1 patient, catheterization of the stenotic aortic valve was not technically feasible.

No differences were seen for the aortic valve area among the different methods (invasive, 0.60 cm^2, range 0.30 to 0.83; MRI, 0.60 cm^2, range 0.30 to 0.80 cm^2; Doppler, 0.60 cm^2, range 0.37 to 0.80; 3D TTE, 0.54 cm^2, range 0.32 to 0.83 cm^2; repeated measures analysis of variance, $p = 0.506$). The Bland-Altman analysis of each noninvasive method compared to catheterization is depicted in Figure 4.

The results of measurements of the aortic root and aortic valve annulus are listed in Table 1. A significant difference in the aortic valve annulus measurements was found among the various methods (e.g., MRI, invasive angiography, TEE, and 2D TTE; Friedman, $p < 0.001$). The measurements of the aortic valve annulus with MRI, TEE, and 2D TTE were larger than with invasive angiography (all comparisons, $p < 0.001$). 2D TTE tended to underestimate the aortic valve annulus diameters compared to TEE and MRI. The aortic valve annulus of 3 patients was beyond the transcatheter aortic valve implantation range using TEE and MRI but not using 2D TTE (Figure 5). The Bland-Altman plots are depicted in Figure 6.

A significant difference was found between the measurements of the aortic sinus (repeated measures analysis of variance, $p = 0.043$), with smaller diameters found with 2D TTE than with MRI ($p = 0.043$). A significant difference was found between the measurements of the sinotubular junction (repeated measures analysis of variance, $p = 0.037$), with smaller diameters found with 2D TTE than with MRI ($p = 0.008$). Also, a significant difference was found between the measurements of the aorta ascendens (Friedman, $p = 0.013$), with smaller diameters found with

Table 1
Individual measurements of mean gradient, left ventricular ejection fraction, left ventricular outflow tract, aortic valve annulus, and aortic root dimensions

Pt. No.	Age (yr)	LVEF (%)	Gradient* (mm Hg)	LVOT (cm)		Aortic Valve Annulus (cm)				Aortic Sinus (cm)			Sinotubular Junction (cm)			Ascending Aorta (cm)		
				MRI	2D TTE	MRI	Invasive	TEE	2D TTE	MRI	Invasive	2D TTE	MRI	Invasive	2D TTE	MRI	Invasive	2D TTE
1	84	78.5	32	2.23	1.83	2.3	1.76	2.45	2.4	3.1	3.04	3.2	2.65	2.67	2.6	2.87	2.8	3.5
2	84	59	84	1.76	1.8	2.51	1.62	2.4	2.3	2.85	2.24	2.7	2.44	2.03	2.3	2.67	2.29	2.8
3	80	74	56	1.92	2	2.2	1.66	2.1	2.4	2.8	2.83	3.1	2.4	2.53	2.4	3.1	2.89	3
4	87	71	34	1.67	1.48	2.2	1.75	2.28	2.1	3	2.66	2.7	2.4	2.12	2.2	2.79	2.7	3.2
5	72	67	45	1.6	1.8	2.5	1.75	2.55	2.3	2.8	3.12	3	2.46	2.54	2.5	3.16	3.4	2.6
6	75	67.5	41	1.84	1.77	2.23	1.83	2.26	2.35	3.36	3.2	3.1	2.82	2.77	2.7	3.31	3.33	2.9
7	87	54	78	1.4	1.59	2.1	2.28	2.1	2.2	3.4	3.75	3.2	3.3	3.06	3.1	3.2	3.54	3.9
8	88	82	45	1.71	1.79	2.4	2.1	2.4	2.31	3.3	3.36	3.3	2.5	2.46	2.53	3.1	3.06	3
9	85	76	27	1.57	1.65	2.35	2.2	2.35	2.4	3.2	3.34	3.2	2.46	2.5	2.6	3.19	2.88	2.3
10	75	28	37	2.23	2.15	3.2	2.96	2.8	2.7	4.3	4.3	3.6	3.2	3.46	3	3.32	3.6	3
11	86	53	31	1.95	2.03	2.67	1.8	2.85	2.5	3.6	2.59	3.2	2.8	2.75	2.45	3.32	3.1	2.5
12	77	76	45	1.42	1.51	2.09	1.86	2.2	2.1	2.76	2.89	2.6	1.9	2.06	1.93	2.85	3.01	2.5
13	85	78	67	1.2	1.1	2.32	2	2.35	2.27	3.1	3	2.96	2.76	2.29	2.37	2.97	3.02	2.7
14	76	62.5	39	2.16	2.04	2.5	1.78	2.5	2.46	3.5	3.14	3.43	2.66	2.3	2.71	2.89	2.89	2.6
15	83	37	33	2.42	2.2	2.8	2.48	2.7	2.59	3.74	4.1	3.75	2.93	2.8	2.47	3.39	3.3	3.3
16	88	53	48	1.98	1.7	2.48	1.77	2.5	2.14	3.2	2.3	2.97	2.2	1.5	2.1	2.75	2.63	2.6
17	67	83	60	1.84	1.7	3.1	2.25	3.1	2.69	3.58	3.4	3.71	3.5	2.98	3.1	3.77	4.18	4
18	87	48	63	2.03	2	2.69	2.2	2.55	2.46	3.47	3.2	3.16	2.8	2.88	2.68	3.39	3.5	2.6
19	83	34	59	2.63	2.44	3	2.62	2.8	2.7	3.58	3.2	3.5	2.9	3	3	3.31	3.16	3
20	80	78	40	1.73	1.7	2.4	1.78	2.4	2.3	3.4	2.77	3.15	2.6	2.09	2.25	3.03	2.99	3.1
21	85	69	38	1.64	1.69	2.85	2.36	2.88	2.81	4.2	3.51	3.53	3.15	2.9	2.92	3.68	3.5	2.9
22	77	69	83	2.05	1.97	2.69	1.8	2.69	2.72	3.6	3.35	3.37	2.98	2.53	2.47	3.01	2.99	2.6
23	84	51	70	1.9	1.8	2.35	1.7	2.35	2.24	3.2	2.78	2.62	2.6	2.25	2.03	2.85	2.87	2.6
24	82	65	38	1.6	1.6	2	2.4	2	2.2	2.7	3.5	3.1	2.2	3.2	2.5	3	3.5	2.4
Median	83.5	67.3	45	1.84	1.80	2.44	1.85	2.43	2.38	3.33	3.17	3.18	2.66	2.54	2.50	3.10	3.04	2.85
Lower	67	28	27	1.20	1.10	2.00	1.62	2.00	2.10	2.70	2.24	2.60	1.90	1.50	1.93	2.67	2.29	2.30
Upper	88	83	84	2.63	2.44	3.20	2.96	3.10	2.81	4.30	4.30	3.75	3.50	3.46	3.10	3.77	4.18	4.00

*Mean transvalvular aortic gradient measured by Doppler ultrasonography.
LVEF = left ventricular ejection fraction measured by MRI; LVOT = left ventricular outflow tract; Pt. No. = patient number.

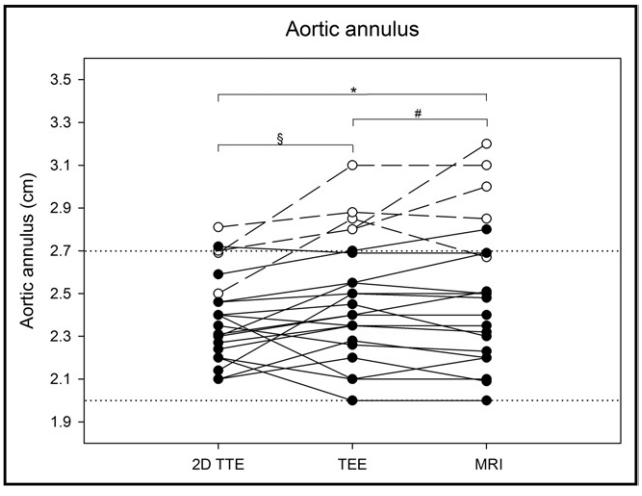

Figure 5. Head-to-head comparison of individual aortic valve annulus diameter measurements by 2D TTE, MRI, and TEE. Transcatheter aortic valve implantation range (CoreValve) displayed (2.0 to 2.7 cm). *Open circles* indicate patients with annulus diameter beyond transcatheter aortic valve implantation range using TEE. 2D TTE tended to underestimate annulus diameters, but all comparisons were not significant after Bonferroni correction (i.e., $p < 0.008$): #p=0.814; *p = 0.025; §p = 0.013.

2D TTE than with MRI ($p = 0.016$). No difference was found between the left ventricular outflow tract measurements using MRI and 2D TTE (p = NS).

The intraobserver reproducibility (mean ± 2 SD) for the assessment of the aortic valve annulus was −0.09 ± 0.18 cm for MRI, −0.27 ± 0.39 cm for invasive angiography, 0.11 ± 0.31 cm for TEE, and −0.03 ± 0.40 cm for 2D TTE. The interobserver reproducibility was −0.12 ± 0.21 cm for MRI, −0.26 ± 0.44 cm for invasive angiography, 0.14 ± 0.30 cm for TEE, and −0.12 ± 0.25 cm for 2D TTE.

Discussion

The results of the present study have demonstrated that in a consecutive series of high-risk, symptomatic patients with severe aortic stenosis, no differences were found in the aortic valve area for MRI planimetry, Doppler echocardiography, 3D TTE, and catheterization. MRI and TEE provided a similar and an essential assessment of the aortic valve annulus dimensions, especially at the limits of the transcatheter aortic valve implantation range. Compared to MRI, the aortic root dimensions were underestimated using 2D TTE.

We compared 2 planimetric aortic valve area measurement methods (steady-state free precession MRI and 3D

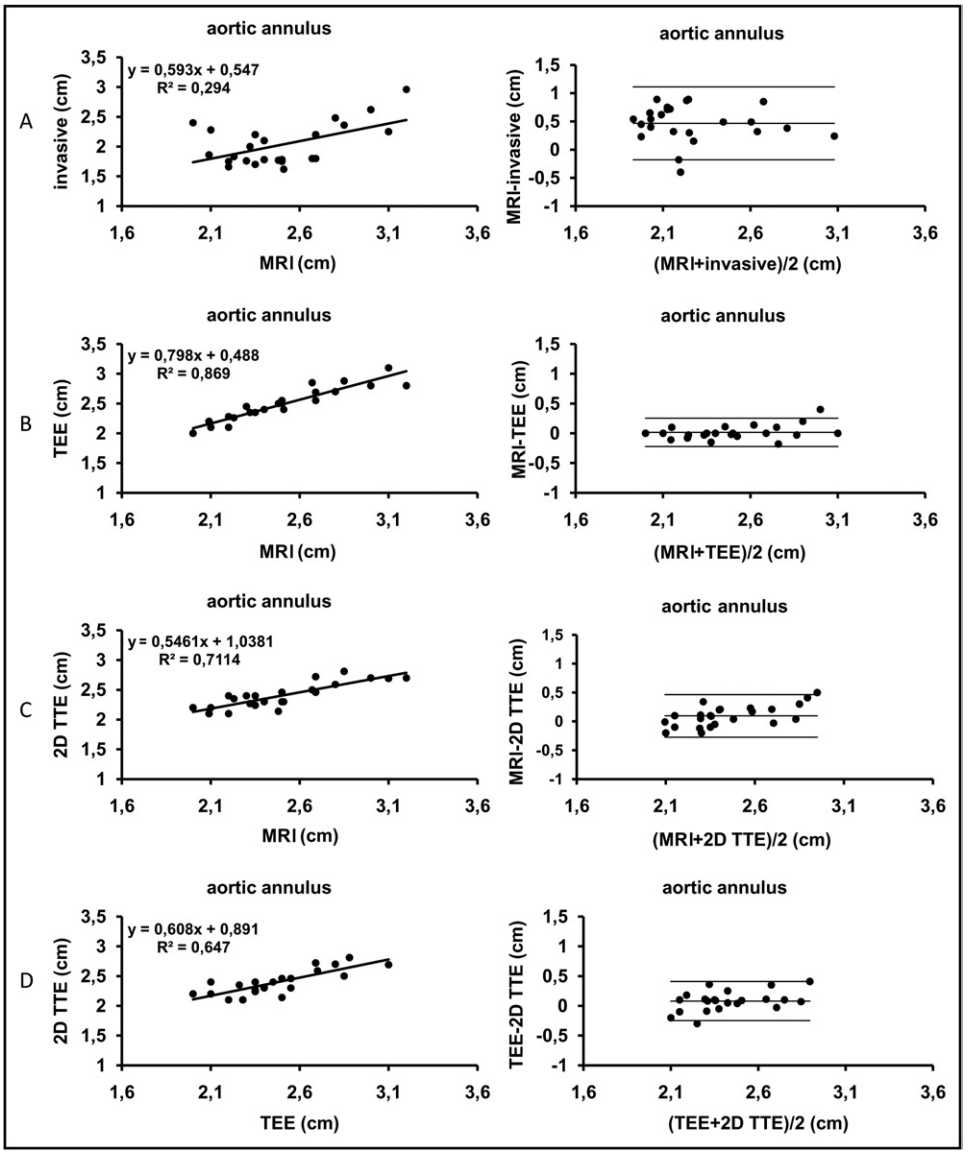

Figure 6. Correlations between MRI and multimodality assessment and correlations between TEE and TTE of aortic valve annulus diameter. Correlation between MRI measured aortic valve annulus diameter and invasive angiography *(A),* TEE *(B),* and 2D TTE *(C).* Correlation between TEE-measured aortic valve annulus diameter and 2D TTE *(D).* Corresponding Bland-Altman plots of difference between MRI-measured aortic valve annulus diameter and invasive angiography *(A),* TEE *(B),* and 2D TTE *(C)* and corresponding Bland-Altman plot of difference between TEE-measured aortic valve annulus and 2D TTE *(D).* Horizontal lines show mean difference between 2 methods ± 2 SDs.

TTE) and calculated the aortic valve area methods (cardiac catheterization using the Gorlin equation and Doppler using the continuity equation). No significant difference was found between these methods. The Bland-Altman analysis demonstrated good agreement between the planimetric (anatomic) and calculated (flow-derived) aortic valve area. In contrast, signal void due to turbulent flow in the area of the aortic valve orifice could have affected MRI planimetry, the irregular shape of the degenerative calcified valves in aortic stenosis could have affected both MRI[7] and 3D TTE planimetric measurements.[8,9] The latter, in particular, applies to 3D TTE, which remains highly dependent on echogenicity when using a transthoracic approach.[10]

Correct aortic valve annulus measurement is crucial to guarantee procedural transcatheter aortic valve implantation success. To allow safe implantation of the CoreValve and the Edwards-Sapien prosthesis, an aortic valve annulus diameter of 20 to 27 mm and 18 to 25 mm is required, respectively. However, a reference standard for aortic valve annulus measurement is lacking. A strategy using the TEE measurements of the aortic valve annulus has already been shown good clinical transcatheter aortic valve implantation results.[10] We found an excellent agreement between the MRI- and TEE-measured aortic valve annulus. However, the annulus diameters tended to be underestimated by 2D TTE compared to TEE and MRI. 2D TTE is commonly affected by suboptimal acoustic windows.[10,11] In a recent study, excluding poor echocardiographic image quality, no difference was found between 2D TTE and TEE.[10] In addition, the aortic valve annulus is not a circular, but a

complex oval 3D, structure with attachment of the aortic leaflets in a crown-like fashion.[12] Therefore, although measurements using different imaging techniques were performed using the long-axis images and aimed to measure the largest diameter of the aortic valve annulus, they might not represent identical anatomic measurements. Three-dimensional TEE and multislice computed tomography offer the advantage of imaging the shape of the aortic valve annulus.[11] Multislice computed tomography has the advantage of providing coronary anatomy but is limited by radiation exposure and the use of iodinated contrast agents at a slow and regular heart rhythm.[10] MRI has the potential of 3D imaging with high spatial resolution using tissue contrast without the need of potentially nephrotoxic contrast agents and without the need for radiation.[13] Invasive angiography displays greater variability for the crucial measurement of aortic valve annulus.[14] Owing to the absence of clear anatomic markers in highly calcified aortic valves, this measurement is rarely performed perpendicular to the aortic valve annulus.[15] Measurements in extensively calcified valves and aortic root can be challenging because of retroacoustic shadowing. Although MRI delineates calcifications as low signal structures permitting precise visualization of the aortic valve, the aortic valve annulus and root even in highly calcified valves,[16] bulky calcifications can limit measurements. When comparing individual measurements, the aortic valve annulus of 3 patients was decreased beyond the transcatheter aortic valve implantation range using TEE and MRI but not 2D TTE. This might indicate that, for the crucial measurement of the aortic valve annulus, multimodal imaging, including TEE and/or MRI, is essential.

Accurate measurement of the aortic root, in general, and the sinotubular junction, in particular, has serious implications for transcatheter aortic valve implantation.[17] Compared to MRI, the aortic root dimensions were underestimated by 2D TTE; however, no significant difference with the invasive measurements was found. 2D TTE is hampered by acoustic windows and scatter in a highly calcified aortic root. TEE is superior to 2D TTE for image quality.[18] Measurements using noninvasive techniques might not represent anatomic measurements identical to those with invasive angiography.[19]

The best method for the assessment of the aortic annulus remains to be determined. Because a reference standard is lacking, additional studies are necessary to define which is the most accurate and the best performing imaging strategy. For correct sizing, integrating different imaging modalities, including TEE, to assess the aortic root anatomy is mandatory in the evaluation of requirements in transcatheter aortic valve implantation selection.

1. Moss RR, Ivens E, Pasupati S, Humphries K, Thompson CR, Munt B, Sinhal A, Webb JG. Role of echocardiography in percutaneous aortic valve implantation. *J Am Coll Cardiol Imaging* 2008;1:15–24.
2. Tops LF, Delgado V, van der Kley F, Bax JJ. Percutaneous aortic valve therapy: clinical experience and the role of multimodality imaging. *Heart* 2009;95:1538–1546.
3. Gorlin R, Gorlin SG. Hydraulic formula for calculation of the area of the stenotic mitral valve, other cardiac valves and central circulatory shunts. I. *Am Heart J* 1951;41:1–29.
4. Skjaerpe T, Hegrenaes L, Hatle L. Noninvasive estimation of valve area in patients with aortic stenosis by Doppler ultrasound and two-dimensional echocardiography. *Circulation* 1985;72:810–818.
5. Paelinck BP, de Roos A, Bax JJ, Bosmans JM, van der Geest RJ, Dhondt D, Parizel PM, Vrints CJ, Lamb HJ. Feasibility of tissue MRI imaging: a pilot study in comparison with Tissue Doppler imaging and invasive measurement. *J Am Coll Cardiol* 2005;45:1109–1116.
6. Bland JM, Altman DG. Statistical methods for assessing agreement between two methods of clinical measurement. *Lancet* 1986;8:307–310.
7. Pouleur AC, le Polain de Waroux JB, Pasquet A, Vanoverschelde JL, Gerber BL. Aortic valve area assessment: multidetector CT compared with cine MRI imaging and transthoracic and transesophageal echocardiography. *Radiology* 2007;244:745–754.
8. John AS, Dill T, Brandt RR, Rau M, Ricken W, Bachmann G, Hamm CW. Magnetic resonance to assess the aortic valve area in aortic stenosis: how does it compare to current diagnostic standards? *J Am Coll Cardiol* 2003;42:519–526.
9. Goland S, Trento A, Lida K. Assessment of aortic stenosis by three-dimensional echocardiography: an accurate and novel approach. *Heart* 2007;93:801–807.
10. Messika-Zeitoun D, Serfaty JM, Brochet E, Ducrocq G, Lepage L, Detaint D, Hyafil F, Himbert D, Pasi N, Laissy JP, Iung B, Vahanian A. Multimodal assessment of the aortic annulus diameter: implications for transcatheter aortic valve implantation. *J Am Coll Cardiol* 2010;55:186–194.
11. Ng AC, Delgado V, van der Kley F, Shanks M, van de Veire NR, Bertini M, Nucifora G, van Bommel RJ, Tops LF, de Weger A, Tavilla G, de Roos A, Kroft LJ, Leung DY, Schuijf J, Schalij MJ, Bax JJ. Comparison of aortic root dimensions and geometrics pre- and post-transcatheter aortic valve implantation by 2-and 3-dimensional transesophageal echocardiography and multi-slice computed tomography. *Circ Cardiovasc Img* 2010;3:94–102.
12. Piazza N, De Jaegere P, Schultz C, Becker AB, Serruys PW, Anderson RH. Anatomy of the aortic valvar complex and its implications for transcatheter implantation of the aortic valve. *Circ Cardiovasc Intervent* 2008;1:74–81.
13. Paelinck BP, Lamb HJ, Bax JJ, Van der Wall EE, de Roos A. Assessment of diastolic function by cardiovascular magnetic resonance. *Am Heart J* 2002;144:198–205.
14. Tzikas A, Schultz CJ, Piazza N, Moelker A, Van Mieghem NM, Nuis RJ, van Geuns RJ, Geleijnse ML, Serruys PW, de Jaegere PPT. Assessment of the aortic annulus by multi-slice computed tomography, contrast aortography and trans-thoracic echocardiography in patients referred for transcatheter aortic valve implantation. *Catheter Cardiovasc Interv* Epub 2010 Sept 7.
15. Kurra V, Kapadia SR, Tuzcu EM, Halliburton SS, Svensson L, Roselli EE, Schoenhagen P. Pre-procedural imaging of aortic root orientation and dimensions: comparison between x-ray angiographic planar imaging and 3-dimensional multidetector row computed tomography. *JACC Cardiovasc Interv* 2010;3:105–113.
16. Tuzcu EM, Kapadia SR, Schoenhagen P. Multimodality quantitative imaging of aortic root for transcatheter aortic valve implantation: more complex than it appears. *J Am Coll Cardiol* 2010;55:195–197.
17. Vahanian A, Alfieri O, Al-Attar N, Antunes M, Bax J, Cormier B, Cribier A, De Jaegere P, Fournial G, Kappetein AP, Kovac J, Ludgate S, Maisano F, Moat N, Mohr F, Nataf P, Piérard L, Pomar JL, Schofer J, Tornos P, Tuzcu M, van Hout B, Von Segesser LK, Walther T. Trancatheter valve implantation for patients with aortic stenosis: a position statement from the European Association of Cardio-Thoracic Surgery (EACTS) and the European Society of Cardiology (ESC), in collaboration with the European Society of Percutaneous Cardiovascular Interventions (EAPCI). *Eur Heart J* 2008;29:1463–1470.
18. Chin D. Echocardiography for transcatheter aortic valve implantation. *Eur J Echocardiogr* 2009;10:i21–i29.
19. Burman E, Keegan J, Kilner P. Aortic root measurement by cardiovascular magnetic resonance: specification of planes and lines of measurement, and corresponding normal values. *Circ Cardiovasc Img* 2008;1:104–113.